bioRxiv preprint doi: https://doi.org/10.1101/2023.01.13.524026; this version posted January 14, 2023. The copyright holder for this preprint (which was not certified by peer review) is the author/funder, who has granted bioRxiv a license to display the preprint in perpetuity. It is made available under aCC-BY-NC-ND 4.0 International license.

1 # ***Listeria monocytogenes* requires DHNA-dependent intracellular redox**
2 **homeostasis facilitated by Ndh2 for survival and virulence**

3

4 Hans B. Smith[1], Kijeong Lee[1], David M. Stevenson[2], Daniel Amador-Noguez[2], John-
5 Demian Sauer[1#]

6

7 [1]Department of Medical Microbiology and Immunology, University of Wisconsin-
8 Madison, Madison, WI, 53706, United States of America
9 [2]Department of Bacteriology, University of Wisconsin-Madison, Madison, WI, 53706,
10 United States of America

11

12 [#]Corresponding author: John-Demian Sauer, Department of Medical Microbiology and
13 Immunology, University of Wisconsin-Madison, Madison, WI, 53706. Phone: (608) 263-
14 1529.
15 E-mail: sauer3@wisc.edu.

16

17 Key Words: *Listeria monocytogenes*, 1,4-dihydroxy-2-naphthoate, menaquinone, redox
18 homeostasis, extracellular electron transfer, Ndh2

19

20 **RUNNING TITLE:** Ndh2 utilizes DHNA to maintain redox homeostasis

bioRxiv preprint doi: https://doi.org/10.1101/2023.01.13.524026; this version posted January 14, 2023. The copyright holder for this preprint (which was not certified by peer review) is the author/funder, who has granted bioRxiv a license to display the preprint in perpetuity. It is made available under aCC-BY-NC-ND 4.0 International license.

21 **ABSTRACT**

22 *Listeria monocytogenes* is a remarkably well-adapted facultative intracellular pathogen
23 that can thrive in a wide range of ecological niches. *L. monocytogenes* maximizes its
24 ability to generate energy from diverse carbon sources using a respiro-fermentative
25 metabolism that can function under both aerobic and anaerobic conditions. Cellular
26 respiration maintains redox homeostasis by regenerating NAD^+ while also generating a
27 proton motive force (PMF). The end products of the menaquinone (MK) biosynthesis
28 pathway are essential to drive both aerobic and anaerobic cellular respiration. We
29 previously demonstrated that intermediates in the MK biosynthesis pathway, notably
30 1,4-dihydroxy-2-naphthoate (DHNA), are required for the survival and virulence of *L.*
31 *monocytogenes* independent of their role in respiration. Furthermore, we found that
32 restoration of NAD^+/NADH ratio through expression of water-forming NADH oxidase
33 (NOX) could rescue phenotypes associated with DHNA deficiency. Here we extend
34 these findings to demonstrate that endogenous production or direct supplementation of
35 DHNA restored both the cellular redox homeostasis and metabolic output of
36 fermentation in *L. monocytogenes*. Further, exogenous supplementation of DHNA
37 rescues the *in vitro* growth and *ex vivo* virulence of *L. monocytogenes* DHNA-deficient
38 mutants. Finally, we demonstrate that exogenous DHNA restores redox balance in *L.*
39 *monocytogenes* specifically through the recently annotated NADH dehydrogenase
40 Ndh2, independent of the extracellular electron transport (EET) pathway. These data
41 suggest that the production of DHNA may represent an additional layer of metabolic
42 adaptability by *L. monocytogenes* to drive energy metabolism in the absence of
43 respiration-favorable conditions.

bioRxiv preprint doi: https://doi.org/10.1101/2023.01.13.524026; this version posted January 14, 2023. The copyright holder for this preprint (which was not certified by peer review) is the author/funder, who has granted bioRxiv a license to display the preprint in perpetuity. It is made available under aCC-BY-NC-ND 4.0 International license.

44 **INTRODUCTION**

45 *Listeria monocytogenes* is a Gram-positive, facultative intracellular pathogen that
46 is exceptionally well-adapted to survive and replicate in the restrictive mammalian host
47 cytosol (1-3). Bacteria that lack the specific adaptations required to survive or replicate
48 in the host niche are effectively cleared (4-7), often by triggering host defense
49 mechanisms comprised of innate immune pathways (8-13). *L. monocytogenes* utilizes
50 its internalin proteins to facilitate invasion into the host cell where it becomes captured
51 in a phagosome (14, 15). The pore-forming cytolysin listeriolysin O (LLO) then facilitates
52 escape from the phagosome into the cytosol (14, 16), where *L. monocytogenes* can
53 utilize ActA to mediate actin-based motility by hijacking the host's actin machinery (17-
54 20). Using this motility, *L. monocytogenes* moves into adjacent cells where they again
55 invade the cytosol by expressing LLO and two phospholipase Cs, PlcA and PlcB,
56 enabling it to restart its life cycle (14, 21).

57 *L. monocytogenes* can also thrive in a diverse range of ecological niches that
58 contain highly variable pools of fermentable and non-fermentable carbon sources (2,
59 22). *L. monocytogenes* employs both fermentative and respiratory metabolic
60 mechanisms to maximize its energy output from scavenged nutrients (22, 23). In
61 contrast to canonical respiratory organisms however, *L. monocytogenes* contains an
62 incomplete tricarboxylic acid (TCA) cycle and is therefore unable to fully oxidize its
63 carbon substrates (24). Accordingly, *L. monocytogenes* utilizes a respiro-fermentative
64 metabolism characterized by glycolysis-derived pyruvate that is funneled into the
65 fermentative production of acetate, generating ATP through substrate-level
66 phosphorylation (SLP) via the activity of acetate kinase (24, 34). During the respiro-

bioRxiv preprint doi: https://doi.org/10.1101/2023.01.13.524026; this version posted January 14, 2023. The copyright holder for this preprint (which was not certified by peer review) is the author/funder, who has granted bioRxiv a license to display the preprint in perpetuity. It is made available under aCC-BY-NC-ND 4.0 International license.

67 fermentative process, the activity of *L. monocytogenes*' respiratory electron transport
68 chain (ETC) enables it to regenerate NAD^+, without having to rely upon lactate
69 dehydrogenase, while also producing a functional proton motive force (PMF) (22, 24,
70 34). Further lending to its diverse metabolic adaptability, *L. monocytogenes* possesses
71 two distinct respiratory ETCs that allow it to respire both aerobically and anaerobically
72 (25). The aerobic ETC in *L. monocytogenes* mediates electron transfer from a type II
73 NADH dehydrogenase, Ndh1, to a membrane-bound menaquinone (MK) and
74 subsequently to terminal cytochrome oxidases QoxAB (aa3) or CydAB (bd) for final
75 transfer to O_2 (26, 27). In contrast, the recently annotated anaerobic respiratory
76 pathway in *L. monocytogenes* uses a flavin-based ETC to drive extracellular electron
77 transfer (EET) to extracytosolic acceptors such as fumarate or ferric ion using a novel
78 NADH dehydrogenase (Ndh2) and an alternative demethylmenaquinone (DMK)
79 intermediate (25, 28). Both of the respiratory ETC in *L. monocytogenes* rely upon the
80 MK biosynthesis pathway to generate their respective quinone electron acceptors, with
81 the biosynthetic intermediate 1,4-dihydroxy-2-naphthoate (DHNA) functioning as a
82 mutual branching point (**Fig. S1**) (25).
83 The requirement for *L. monocytogenes* to perform cellular respiration during
84 infection has been well documented (29-32). However, understanding the specific
85 contributions of maintaining cellular redox homeostasis via NAD^+ regeneration versus
86 the production of a functional PMF to achieve virulence has remained elusive. Further
87 complicating our ability to dissect the specific contributions that cellular respiration may
88 have during infection, the MK intermediates DHNA-CoA and DHNA have recently been
89 reported to be required for the survival and virulence of *L. monocytogenes* independent

bioRxiv preprint doi: https://doi.org/10.1101/2023.01.13.524026; this version posted January 14, 2023. The copyright holder for this preprint (which was not certified by peer review) is the author/funder, who has granted bioRxiv a license to display the preprint in perpetuity. It is made available under aCC-BY-NC-ND 4.0 International license.

90 of MK synthesis and aerobic respiration (29, 31, 32). Importantly, although it was
91 observed that the supplementation of exogenous DHNA could rescue the *in vitro* growth
92 of a DHNA-deficient *L. monocytogenes* mutant, this rescue did not coincide with the
93 restoration of its PMF (31). Therefore, although DHNA-deficient strains of *L.*
94 *monocytogenes* possess the downstream enzymes to produce MK or DMK, these data
95 suggest that exogenous DHNA is not utilized to promote either aerobic or anaerobic
96 cellular respiration. Recent work from Rivera-Lugo *et al.* sought to dissect the relative
97 importance of maintaining redox homeostasis versus PMF generation for the
98 pathogenesis of *L. monocytogenes* using a water-forming NADH oxidase (NOX) that
99 specifically regenerates NAD^+ independent of respiration and PMF function (34).
100 Through the heterologous expression of NOX in respiration-deficient strains of *L.*
101 *monocytogenes*, it was concluded that the regeneration of NAD^+ represents a major role
102 for cellular respiration during pathogenesis.
103 The studies presented here sought to define the respiration-independent
104 mechanisms of DHNA utilization to promote the survival and virulence of *L.*
105 *monocytogenes*. Consistent with observations from Rivera-Lugo *et. al*, in the absence of
106 respiration, the *ex vivo* and *in vivo* virulence defects associated with DHNA-deficiency
107 were a result of impaired redox homeostasis which could be rescued upon ectopic NOX
108 expression. Similarly, exogenous DHNA supplementation rescues the *in vitro* and *ex*
109 *vivo* growth and cytosolic survival of DHNA-deficient mutants. Indeed, DHNA-dependent
110 rescue by direct supplementation resulted in a restored cellular redox homeostasis with
111 a concurrent shift of fermentative flux from lactate production to acetate in *L.*
112 *monocytogenes*, independent of respiration. We further go on to show that the recently

bioRxiv preprint doi: https://doi.org/10.1101/2023.01.13.524026; this version posted January 14, 2023. The copyright holder for this preprint (which was not certified by peer review) is the author/funder, who has granted bioRxiv a license to display the preprint in perpetuity. It is made available under aCC-BY-NC-ND 4.0 International license.

113 annotated anaerobic-specific Ndh2 is essential for DHNA-deficient *L. monocytogenes*
114 mutants to utilize exogenous DHNA for growth in defined medium, independent of its
115 canonical role in EET, suggesting that Ndh2 is the NADH dehydrogenase specifically
116 required for the restoration of redox homeostasis via DHNA. Taken together, these data
117 suggest that the endogenous production of DHNA can be utilized by *L. monocytogenes*
118 to restore both its intracellular redox homeostasis and fermentative metabolic flux
119 through an undefined mechanism requiring Ndh2.
120

121 **RESULTS**

122 **Redox homeostasis via NOX shifts fermentative output and rescues *in vitro***
123 **growth of DHNA-deficient *L. monocytogenes*.**

124 Two main outcomes of cellular respiration include 1) maintaining intracellular
125 redox homeostasis by regenerating NAD^+ from NADH and 2) the generation of a PMF
126 to drive oxidative phosphorylation and various other aspects of bacterial physiology. A
127 recent study employed a water-forming NADH oxidase (NOX) expression system in *L.*
128 *monocytogenes* to dissect the relative importance of cellular respiration in maintaining
129 redox homeostasis versus PMF generation (34). We had previously demonstrated that
130 *L. monocytogenes* mutants lacking the key MK biosynthetic intermediate DHNA were
131 attenuated, in part, independent of loss of respiration (29, 31, 32). We hypothesized that
132 restoration of NAD^+ pools might rescue these virulence defects similar to the rescue
133 observed for mutants lacking components of the respiratory chains (34). To test this
134 hypothesis, we assessed NAD^+/NADH levels in Δ*menB*, Δ*menI* and Δ*menA* mutants +/-
135 expression of NOX *in trans*. The inability to generate endogenous DHNA by the Δ*menB*

bioRxiv preprint doi: https://doi.org/10.1101/2023.01.13.524026; this version posted January 14, 2023. The copyright holder for this preprint (which was not certified by peer review) is the author/funder, who has granted bioRxiv a license to display the preprint in perpetuity. It is made available under aCC-BY-NC-ND 4.0 International license.

136 mutant results in a severely diminished redox homeostasis as measured by the ratio of
137 oxidized NAD^+ to reduced NADH. This imbalance was significantly restored by ectopic
138 expression of NOX to a level similar to the Δ*menA* mutant (**Fig. 1A**). The Δ*menI* mutant,
139 which can generate DHNA-CoA, displays an intermediate phenotype between Δ*menB*
140 and Δ*menA* levels, which is similarly rescued upon NOX expression (**Fig. 1A**),
141 consistent with possible respiration independent roles for DHNA in NAD^+/NADH redox
142 balancing.

143 *L. monocytogenes* employs a respiro-fermentative metabolism due to an
144 incomplete TCA cycle, characterized by the funneling of pyruvate towards the
145 fermentative production of acetate (23, 24). Respiration-deficient mutants of *L.*
146 *monocytogenes* are impaired in their ability to maintain cellular redox homeostasis and
147 as a result nearly exclusively produce lactate rather than acetate as a metabolic
148 byproduct (34). To test whether impaired redox homeostasis due to DHNA-deficiency
149 would similarly result in the predominant production of lactate, we analyzed
150 fermentation byproducts in bacterial supernatants using high-performance liquid
151 chromatography (HPLC). As expected, wild-type *L. monocytogenes* predominantly
152 generated acetate whereas DHNA-deficient Δ*menB* had a drastic shift to lactate
153 production (**Fig. 1B**). Heterologous NOX expression rescued Δ*menB* acetate production
154 back to wild-type levels, consistent with restored redox homeostasis driving acetate
155 production to generate ATP (**Fig. 1B**). Consistent with the results seen in our
156 NAD^+/NADH experiments, the Δ*menI* mutant displayed an intermediate phenotype by
157 producing similar levels of acetate and lactate, which was also fully restored to wild-type
158 upon NOX expression (**Fig. 1B**). The Δ*menA* mutant produced slightly more lactate and

bioRxiv preprint doi: https://doi.org/10.1101/2023.01.13.524026; this version posted January 14, 2023. The copyright holder for this preprint (which was not certified by peer review) is the author/funder, who has granted bioRxiv a license to display the preprint in perpetuity. It is made available under aCC-BY-NC-ND 4.0 International license.

159 less acetate when compared to wild-type, likely attributed to the difference in redox
160 homeostasis observed previously (**Fig. 1A, B**).
161 Finally, we have previously shown that the production of DHNA is critical for *L.*
162 *monocytogenes in vitro* growth in chemically defined medium (29, 31, 32). To test
163 whether restoration of redox homeostasis can rescue this growth defect, we've assayed
164 for *in vitro* growth of the above mutants complemented with NOX in defined medium. As
165 expected, Δ*menB* showed the largest growth defect followed by Δ*menI*, and both
166 mutants showed wild-type level growth upon NOX complementation (**Fig. 1C**).
167 Together, these data suggest that metabolic defects associated with DHNA deficiency
168 in *L. monocytogenes* are due to NAD^+/NADH redox imbalances and that restoration of
169 this balance can rescue Δ*menB* mutant growth and carbon metabolism in *L.*
170 *monocytogenes*.
171

172 **Restoration of redox homeostasis rescues virulence defects associated with**
173 **DHNA-deficiency.**
174 Based on the restoration of *in vitro* growth of Δ*menB* mutants via expression of
175 NOX, we hypothesized that restoration of NAD^+ pools would similarly rescue virulence
176 defects of DHNA-deficient mutants. DHNA-deficient mutants are susceptible to cytosolic
177 killing in the macrophage cytosol, therefore we assessed cytosolic survival of Δ*menB*,
178 Δ*menI*, and Δ*menA* with or without expression of NOX *in trans* (29, 35). As
179 hypothesized, Δ*menB* and Δ*menI* displayed increased cytosolic killing and NOX
180 expression rescued their survival in the macrophage cytosol (**Fig. 2A**). Rescue by NOX

bioRxiv preprint doi: https://doi.org/10.1101/2023.01.13.524026; this version posted January 14, 2023. The copyright holder for this preprint (which was not certified by peer review) is the author/funder, who has granted bioRxiv a license to display the preprint in perpetuity. It is made available under aCC-BY-NC-ND 4.0 International license.

181 expression was specific to mutants with disrupted NAD^+/NADH redox homeostasis as
182 NOX expression was unable to rescue cytosolic survival of a Δ*glmR* mutant susceptible
183 to cytosolic killing due to cell wall defects (**Fig 2A**) (33, 35, 36). Consistent with NAD^+
184 pool restoration supporting cytosolic survival, Δ*menB* mutant replication in the
185 macrophage cytosol was also rescued upon expression of NOX *in trans* (**Fig. 2B**).

186 Finally, we had previously demonstrated that DHNA-deficient mutants are more
187 attenuated *in vivo* than respiration-deficient mutants, suggesting that DHNA contributes
188 to virulence in a respiration independent manner (29, 31, 32). To determine if the
189 respiration independent function of DHNA during *in vivo* infection is due to NAD^+/NADH
190 homeostasis defects, we assessed virulence of Δ*menB*, Δ*menI*, and Δ*menA* mutant *L.*
191 *monocytogenes* with and without expression of NOX *in trans*. Ectopic NOX expression
192 rescued the *in vivo* burden of Δ*menB* mutants by ~100-fold in the spleen and liver (**Fig.**
193 **2C**) and a similar rescue for Δ*menI* mutants in the liver following NOX expression is also
194 observed (**Fig. 2C**). Interestingly, there was little to no change in the *in vivo* virulence of
195 Δ*menA* upon the introduction of NOX (**Fig 2C**). This is in agreeance with our previous
196 results that showed both redox homeostasis and acetate production of the Δ*menA*
197 mutant was also not significantly altered upon NOX expression (**Fig 1A, B**). Taken
198 together, these data suggest that in *L. monocytogenes* maintaining cellular redox
199 homeostasis in the absence of DHNA is sufficient to promote survival and virulence
200 both *ex vivo* and *in vivo*.

201

202 **DHNA production or supplementation promotes similar effects to NOX**
203 **complementation in *L. monocytogenes*.**

bioRxiv preprint doi: https://doi.org/10.1101/2023.01.13.524026; this version posted January 14, 2023. The copyright holder for this preprint (which was not certified by peer review) is the author/funder, who has granted bioRxiv a license to display the preprint in perpetuity. It is made available under aCC-BY-NC-ND 4.0 International license.

204 We have previously demonstrated that exogenous addition of either purified
205 DHNA or culture supernatant from DHNA sufficient strains of *L. monocytogenes* could
206 rescue the *in vitro* growth of DHNA-deficient *L. monocytogenes* in defined media (31),
207 suggesting that *L. monocytogenes*, like other bacteria including *Propionibacterium* spp.
208 and *Lactobacillus* spp., may secrete DHNA (43, 45). To test the hypothesis that *L.*
209 *monocytogenes* secretes DHNA, we assayed culture supernatants for DHNA via mass
210 spectrometry. As hypothesized, wild-type *L. monocytogenes* contained abundant levels
211 of DHNA, while Δ*menB* mutants contained no detectable extracellular DHNA (**Fig. S2)**.
212 Given that exogenous DHNA could rescue the *in vitro* growth of DHNA-deficient *L.*
213 *monocytogenes* mutants and that DHNA-deficient mutants could similarly be rescued by
214 NAD^+ regeneration through NOX expression, we hypothesized that exogenous DHNA
215 could act to restore NAD^+ levels in Δ*menB* mutants. To test this hypothesis, we
216 measured cellular NAD^+/NADH with or without DHNA supplementation. Consistent with
217 the results observed with NOX expression, the exogenous supplementation of DHNA
218 rescued redox homeostasis of Δ*menB* mutants to levels similar to those seen with
219 Δ*menA* mutants, suggesting that exogenous DHNA might be utilized in a similar fashion
220 to DHNA produced endogenously (**Fig. 3A**). Consistent with DHNA supplementation of
221 Δ*menB* rescuing cellular redox homeostasis, exogenous DHNA also shifted the
222 metabolic flux of Δ*menB* back towards acetate production, similar to Δ*menA* levels (**Fig.**
223 **3B**). Importantly, we had previously demonstrated that exogenous DHNA does not
224 restore respiration and membrane potential (31). Taken together, these data suggest
225 that DHNA, independent of its role in respiration, restores cellular redox homeostasis,

bioRxiv preprint doi: https://doi.org/10.1101/2023.01.13.524026; this version posted January 14, 2023. The copyright holder for this preprint (which was not certified by peer review) is the author/funder, who has granted bioRxiv a license to display the preprint in perpetuity. It is made available under aCC-BY-NC-ND 4.0 International license.

226 subsequently shifting the fermentative output from lactate back towards acetate that
227 likely drives ATP production through acetate kinase (24, 34).
228 Having previously observed that DHNA can restore NAD^+ redox homeostasis
229 and that NOX-dependent NAD^+ restoration could restore virulence defects of Δ*menB*
230 mutants, we hypothesized that exogenous DHNA supplementation during infection may
231 similarly rescue the cytosolic survival and intracellular growth of DHNA-deficient *L.*
232 *monocytogenes*. Indeed, the addition of exogenous DHNA during macrophage infection
233 with Δ*menB* or Δ*menI* mutants restored their cytosolic survival back to wild-type and
234 Δ*menA* levels (**Fig. 3C**). Importantly, as observed with NOX expression, DHNA
235 supplementation did not rescue the cytosolic survival of Δ*glmR* mutants whose
236 virulence phenotypes are due to cell wall stress response defects (**Fig. 3C**) (33, 36),
237 demonstrating that the rescue of cytosolic survival by DHNA is specific to DHNA-
238 deficient *L. monocytogenes*. Accordingly, supplementing DHNA during macrophage
239 infection also rescued the ability of Δ*menB* mutants to replicate intracellularly to levels
240 similar of that during Δ*menA* infection (**Fig 3D**). Taken together, these results
241 demonstrate that exogenously provided DHNA can balance NAD^+/NADH redox
242 homeostasis thereby potentiating *L. monocytogenes* virulence.
243

244 ***ndh2* is conditionally essential for DHNA utilization *in vitro*.**

245 Although DHNA can drive regeneration of NAD^+ in *L. monocytogenes* upon
246 exogenous supplementation, it does not restore membrane potential suggesting that it
247 is not simply imported and used to synthesize MK as described in Streptococci (44, 53).
248 We hypothesized that the two annotated *L. monocytogenes'* NADH dehydrogenases

bioRxiv preprint doi: https://doi.org/10.1101/2023.01.13.524026; this version posted January 14, 2023. The copyright holder for this preprint (which was not certified by peer review) is the author/funder, who has granted bioRxiv a license to display the preprint in perpetuity. It is made available under aCC-BY-NC-ND 4.0 International license.

249 encoded by *ndh1* (*LMRG_02734*) and *ndh2* (*LMRG_02183*), respectively, may utilize
250 DHNA independent of the respiratory pathways to facilitate NAD^+/NADH homeostasis
251 (23, 25). To test this hypothesis, we generated Δ*ndh1*/*menB*::Tn and *ndh2*::Tn/Δ*menB*
252 mutants and assayed for growth with or without 5μM exogenous DHNA in defined
253 medium. As expected, both double mutants were unable to grow without exogenous
254 DHNA due them being a Δ*menB* mutant (**Fig. 4A**). DHNA supplementation rescued
255 growth of the Δ*ndh1*/*menB*::Tn mutant suggesting that Ndh1 is not required for DHNA-
256 dependent NAD^+/NADH redox homeostasis. In contrast, the *ndh2*::Tn/Δ*menB* mutant
257 was unable to grow in the presence of exogenous DHNA (**Fig. 4B**). *ndh2* is required for
258 the function of the recently described EET pathway in *L. monocytogenes* (25), therefore
259 we hypothesized that EET may be necessary to utilize DHNA for NAD^+/NADH redox
260 homeostasis. To test this hypothesis, we transduced *pplA*::Tn, *dmkA*::Tn, *eetA*::Tn, and
261 *fmnA*::Tn mutations into a Δ*menB* background. The growth of all four of these double
262 mutants were rescued upon DHNA supplementation in defined medium (**Fig. S3**).
263 Finally, exogenous MK supplementation can restore not only growth of DHNA deficient
264 mutants but also their membrane potential (31, 32), likely through direct insertion of MK
265 in the membrane and subsequent restoration of the aerobic respiratory chain. To ensure
266 that *ndh2*::Tn/Δ*menB* mutants are not more generally incapable of growing in defined
267 media, we supplemented *ndh2*::Tn/Δ*menB* mutants with either DHNA or MK directly.
268 Supplementation of MK rescued growth of *ndh2*::Tn/Δ*menB* in defined medium unlike
269 DHNA, showing that this mutant is specifically dysfunctional in the use of DHNA as a
270 redox homeostasis substrate (**Fig. 4C**). Taken together, these data suggest that Ndh2

bioRxiv preprint doi: https://doi.org/10.1101/2023.01.13.524026; this version posted January 14, 2023. The copyright holder for this preprint (which was not certified by peer review) is the author/funder, who has granted bioRxiv a license to display the preprint in perpetuity. It is made available under aCC-BY-NC-ND 4.0 International license.

271 facilitates DHNA-dependent NAD^+/NADH redox homeostasis in the absence of
272 respiration in *L. monocytogenes*.

273 **DISCUSSION**

274 Cytosolic pathogens require specific adaptations to survive and replicate within
275 the host. In *L. monocytogenes*, MK biosynthetic intermediate DHNA is among those
276 factors necessary for cytosolic survival, independent of its known role in MK synthesis
277 and cellular respiration (29, 31). In the present study, we sought to address the
278 respiration-independent mechanism by which DHNA is required for the survival and
279 virulence of *L. monocytogenes*. Utilizing a heterologous NOX expression system, we
280 demonstrated that virulence defects associated with loss of DHNA could be rescued by
281 restoration of NAD^+/NADH homeostasis (**Fig. 1, 2**). We then found that exogenous
282 DHNA supplementation restores NAD^+/NADH balance, cytosolic survival, and
283 intracellular replication of the DHNA-deficient mutant Δ*menB* (**Fig.3**). Balancing of redox
284 homeostasis also coincided with a marked shift in fermentative flux from lactate to
285 acetate upon DHNA production or supplementation (**Fig. 3B**) to maximize ATP
286 production via SLP through the activity of acetate kinase (34, 37). Lastly, we provide
287 evidence that Ndh2 is the NADH dehydrogenase responsible for restoring redox
288 homeostasis during extracellular DHNA utilization, independent of its role in EET (**Fig.**
289 **4**).

290 Although we've demonstrated that Ndh2 is conditionally essential for DHNA
291 utilization in *L. monocytogenes*, it is still unclear how Ndh2 utilizes DHNA to maintain
292 intracellular redox homeostasis. One possibility is that DHNA, or one of its derivatives,

bioRxiv preprint doi: https://doi.org/10.1101/2023.01.13.524026; this version posted January 14, 2023. The copyright holder for this preprint (which was not certified by peer review) is the author/funder, who has granted bioRxiv a license to display the preprint in perpetuity. It is made available under aCC-BY-NC-ND 4.0 International license.

293 may be used as an alternative quinone to directly accept electrons from Ndh2,
294 regenerating NAD^+ similar to the system recently described in *Shewanella oneidensis*
295 MR-1. Mevers *et al*. recently demonstrated that a derivative of DHNA, 2-amino-3-
296 carboxy-1,4-naphthoquinone (ACNQ), could serve as a novel electron shuttle that
297 functioned to promote redox balance and energy metabolism (38). The authors went on
298 to show that ACNQ is produced non-enzymatically from extracellular DHNA under
299 oxidizing conditions in the presence of a nitrogen donor (i.e. ammonium or amino acids)
300 (38). We have confirmed that indeed, DHNA is secreted by wild-type *L. monocytogenes*
301 (**Fig. S2**) and extracellular DHNA is readily converted to ACNQ in our defined medium
302 based on mass spectrometry analysis (data not shown). Based on this model, it is
303 possible that DHNA produced by *L. monocytogenes* is secreted outside of the cell to
304 shuttle electrons away where it is then freely oxidized non-enzymatically in the local
305 environment to form ACNQ. Newly formed ACNQ would then be imported back into *L.*
306 *monocytogenes* to be reduced again through the activity of Ndh2. The repeated
307 oxidation and reduction of DHNA and/or ACNQ is the hallmark of an “electron shuttle”
308 and is one of the proposed mechanisms of EET in *S. oneidensis* (38, 39). A strikingly
309 similar model has been described in *Pseudomonas aeruginosa* in which endogenous
310 production of phenazine is cyclically reduced intracellularly, shuttled outside of the cell,
311 and oxidized by a terminal electron acceptor where it is then imported again by the cell
312 (41). Studies to determine whether DHNA/ACNQ fuels an Ndh2-dependent electron
313 shuttle to maintain intracellular redox homeostasis or whether DHNA works via an
314 alternative mechanism are currently ongoing.

bioRxiv preprint doi: https://doi.org/10.1101/2023.01.13.524026; this version posted January 14, 2023. The copyright holder for this preprint (which was not certified by peer review) is the author/funder, who has granted bioRxiv a license to display the preprint in perpetuity. It is made available under aCC-BY-NC-ND 4.0 International license.

315 It has been proposed that in addition to serving as an electron shuttle by *P.*
316 *aeruginosa,* secreted phenazine may be used as a shared resource by the surrounding
317 microbial community to fuel their own redox shuttling (42). The function of phenazine as
318 a shared metabolite is also similar to what has been previously documented with the
319 secretion of DHNA being used as a shared resource to fuel metabolic processes of
320 other localized microbes (31, 43–45). Furthermore, a recent study by Tejedor-Sanz *et*
321 *al.* reported that the homofermentative lactic acid bacteria *Lactiplantibacillus plantarum*
322 contains the EET gene locus previously annotated in *L. monocytogenes*, however it is
323 missing the upstream genes necessary for quinone biosynthesis (40). Upon addition of
324 exogenous DHNA, *L. plantarum* was observed to employ an Ndh2-dependent form of
325 EET that functioned to increase intracellular redox homeostasis by enhancing metabolic
326 flux through fermentative pathways, generating additional lactate, while increasing ATP
327 generation through SLP (40). Importantly, the capacity of DHNA supplementation to
328 induce EET in *L. plantarum* did not coincide with the generation of a PMF to drive
329 oxidative phosphorylation, similar to the phenotypes observed in *L. monocytogenes*.
330 Whether there are functions of *L. monocytogenes* secreted DHNA as a shared
331 metabolite in complex microbial communities such as those found in the intestine during
332 the early stages of infection will require additional future studies.
333 Overall, we've shown that *L. monocytogenes* can utilize DHNA to maintain redox
334 homeostasis through the anaerobic-specific NADH dehydrogenase Ndh2, independent
335 of other EET proteins. Utilization of extracellular DHNA can aid DHNA-deficient *L.*
336 *monocytogenes* mutants to restore their ability to grow and replicate within the cytosol
337 by potentially driving a yet unclear method of energy metabolism. Pathways involved in

bioRxiv preprint doi: https://doi.org/10.1101/2023.01.13.524026; this version posted January 14, 2023. The copyright holder for this preprint (which was not certified by peer review) is the author/funder, who has granted bioRxiv a license to display the preprint in perpetuity. It is made available under aCC-BY-NC-ND 4.0 International license.

338 unique energy metabolism by various pathogens are increasingly viewed as attractive
339 drug targets and as such future studies utilizing the important model pathogen *L.*
340 *monocytogenes* to understand the mechanisms of DHNA-dependent redox homeostasis
341 could provide novel insights into the generation of new antimicrobials.
342

bioRxiv preprint doi: https://doi.org/10.1101/2023.01.13.524026; this version posted January 14, 2023. The copyright holder for this preprint (which was not certified by peer review) is the author/funder, who has granted bioRxiv a license to display the preprint in perpetuity. It is made available under aCC-BY-NC-ND 4.0 International license.

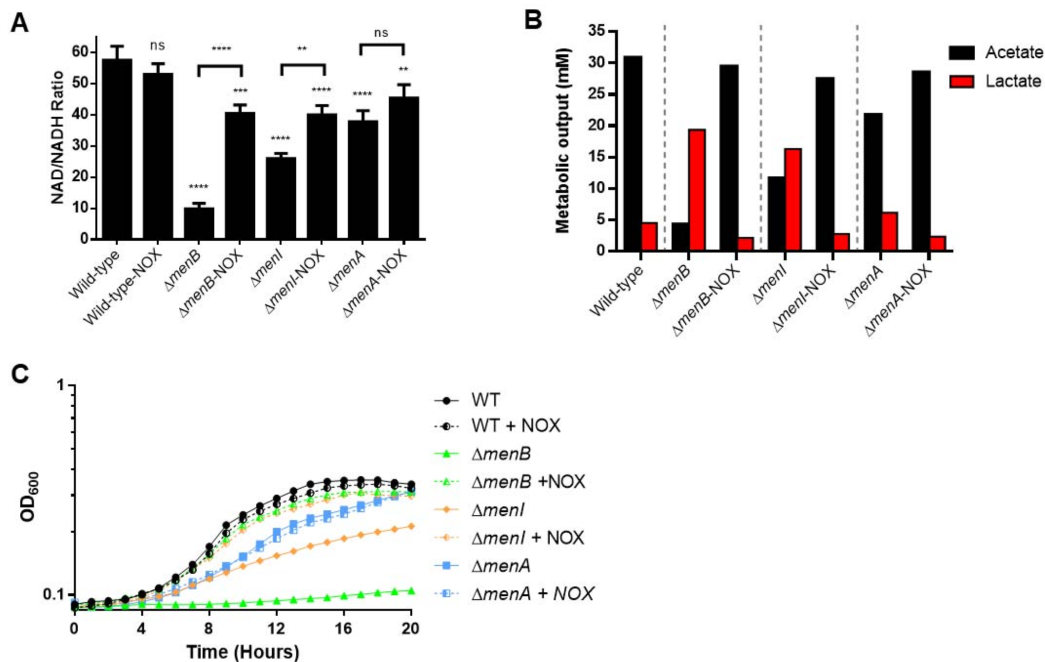

343

344 **Figure 1.** Redox homeostasis via NOX shifts fermentative output and rescues *in vitro*
345 growth of DHNA-deficient *L. monocytogenes*. (A) NAD^+/NADH ratios of indicated *L.*
346 *monocytogenes* strains +/- NOX plasmid complementation grown aerobically at 37°C in
347 defined medium to mid-logarithmic phase (OD_{600} 0.4-0.6). Δ*menB* mutant fails to grow in
348 defined medium, thus these culture samples were spiked with 2 × 10^8 total CFU from an
349 overnight BHI culture during experimental setup. (B) HPLC quantification of
350 fermentation products (Lactate and Acetate) produced and secreted by indicated *L.*
351 *monocytogenes* strains +/- NOX plasmid complementation grown in BHI media
352 aerobically at 37°C to stationary phase. (C) *L. monocytogenes* strains +/- NOX plasmid
353 complementation were grown in defined medium at 37°C. OD_{600} was monitored for 20
354 hours. Data are representative of three (A, C) or two (B) independent experiments. ns,
355 not significant; WT, wild-type

bioRxiv preprint doi: https://doi.org/10.1101/2023.01.13.524026; this version posted January 14, 2023. The copyright holder for this preprint (which was not certified by peer review) is the author/funder, who has granted bioRxiv a license to display the preprint in perpetuity. It is made available under aCC-BY-NC-ND 4.0 International license.

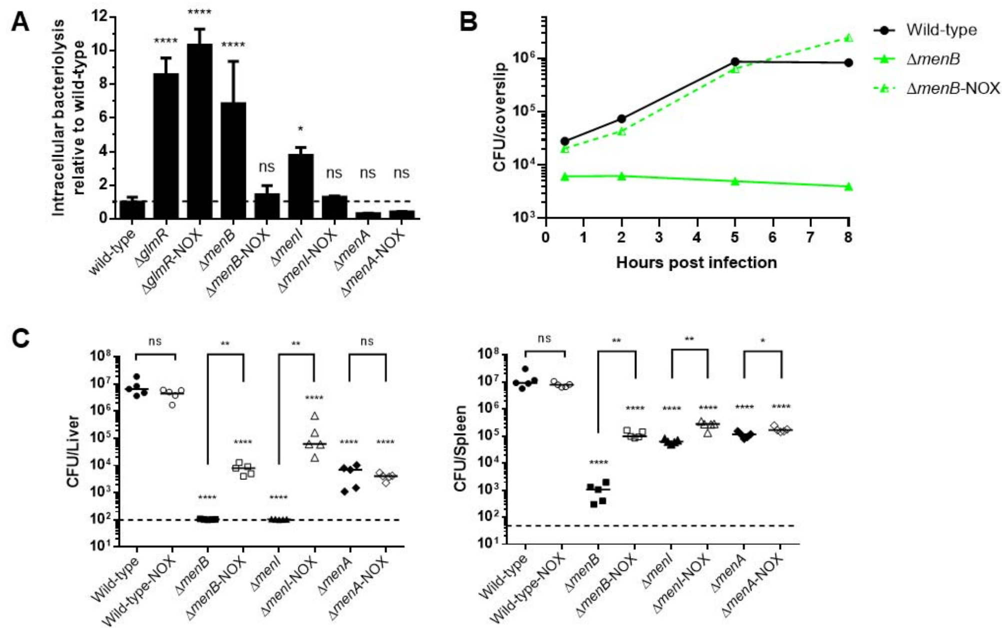

356

357 **Figure 2.** Restoration of redox homeostasis rescues virulence defects associated with

358 DHNA-deficiency. (A) Indicated *L. monocytogenes* strains (MOI of 10) +/- NOX plasmid

359 complementation were tested for cytosolic survival in immortalized IFNAR$^{-/-}$ bone

360 marrow-derived macrophages (BMDM) over a 6 hr infection. Data are normalized to

361 wild-type levels of bacteriolysis and presented as the standard deviation of the means

362 from three independent experiments. (B) Intracellular growth of wild-type, Δ*menB*, or

363 Δ*menB*-NOX was determined in BMDMs following infection at an MOI of 0.2. Growth

364 curves are representative of at least three independent experiments. Error bars

365 represent the standard deviation of the means of technical triplicates within the

366 representative experiment. (C) Bacterial burdens from the spleen and liver were

367 enumerated at 48 hr post-intravenous infection with 1 × 10^5 total CFU of indicated *L.*

368 *monocytogenes* strains +/- NOX plasmid complementation. Data are representative of

369 results from two independent experiments. Horizontal bars represent the limits of

bioRxiv preprint doi: https://doi.org/10.1101/2023.01.13.524026; this version posted January 14, 2023. The copyright holder for this preprint (which was not certified by peer review) is the author/funder, who has granted bioRxiv a license to display the preprint in perpetuity. It is made available under aCC-BY-NC-ND 4.0 International license.

370 detection and the bars associated with the individual strains represents the mean of the
371 group. ns, not significant.
372
373
374
375
376
377
378
379
380
381
382
383

bioRxiv preprint doi: https://doi.org/10.1101/2023.01.13.524026; this version posted January 14, 2023. The copyright holder for this preprint (which was not certified by peer review) is the author/funder, who has granted bioRxiv a license to display the preprint in perpetuity. It is made available under aCC-BY-NC-ND 4.0 International license.

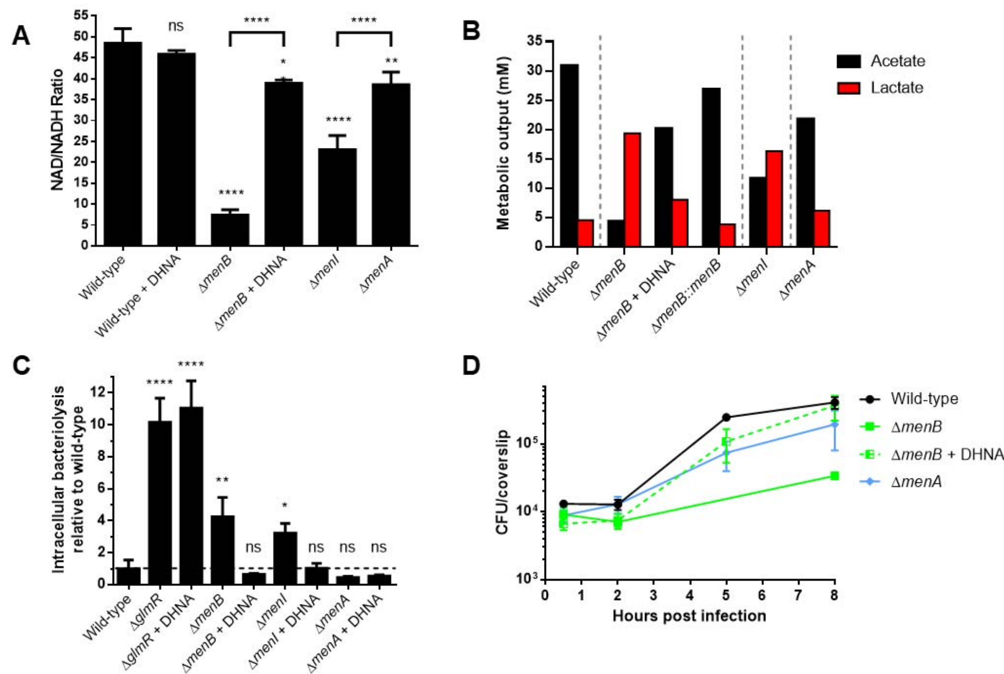

384

385 **Figure 3.** DHNA production or supplementation promotes similar effects to NOX
386 complementation in *L. monocytogenes*. (A) NAD^+/NADH ratios of indicated *L.*
387 *monocytogenes* strains +/- exogenous DHNA supplementation grown aerobically at
388 37°C in defined medium to mid-logarithmic phase. Again, Δ*menB* were spiked with 2 ×
389 10^8 total CFU from an overnight BHI culture during experimental setup. Data are
390 presented as the standard deviation of the means from three independent experiments.
391 (B) HPLC quantification of fermentation products (Lactate and Acetate) produced and
392 secreted by indicated *L. monocytogenes* strains +/- exogenous DHNA supplementation
393 grown in BHI media aerobically at 37°C to stationary phase. Data are representative of
394 two independent experiments. (C) Indicated *L. monocytogenes* strains (MOI of 10) +/-
395 DHNA supplementation were tested for cytosolic survival in primary IFNAR -/- BMDMs
396 over a 6 hr infection. Data are normalized to wild-type levels of bacteriolysis and
397 presented as the standard deviation of the means from three independent experiments.

bioRxiv preprint doi: https://doi.org/10.1101/2023.01.13.524026; this version posted January 14, 2023. The copyright holder for this preprint (which was not certified by peer review) is the author/funder, who has granted bioRxiv a license to display the preprint in perpetuity. It is made available under aCC-BY-NC-ND 4.0 International license.

398 (D) Intracellular growth of wild-type, Δ*menB*, or Δ*menA* was determined in BMDMs
399 following infection at an MOI of 0.2. Growth curves are representative of at least three
400 independent experiments. Error bars represent the standard deviation of the means of
401 technical triplicates within the representative experiment. ns, not significant.
402
403
404
405
406
407
408
409
410
411

bioRxiv preprint doi: https://doi.org/10.1101/2023.01.13.524026; this version posted January 14, 2023. The copyright holder for this preprint (which was not certified by peer review) is the author/funder, who has granted bioRxiv a license to display the preprint in perpetuity. It is made available under aCC-BY-NC-ND 4.0 International license.

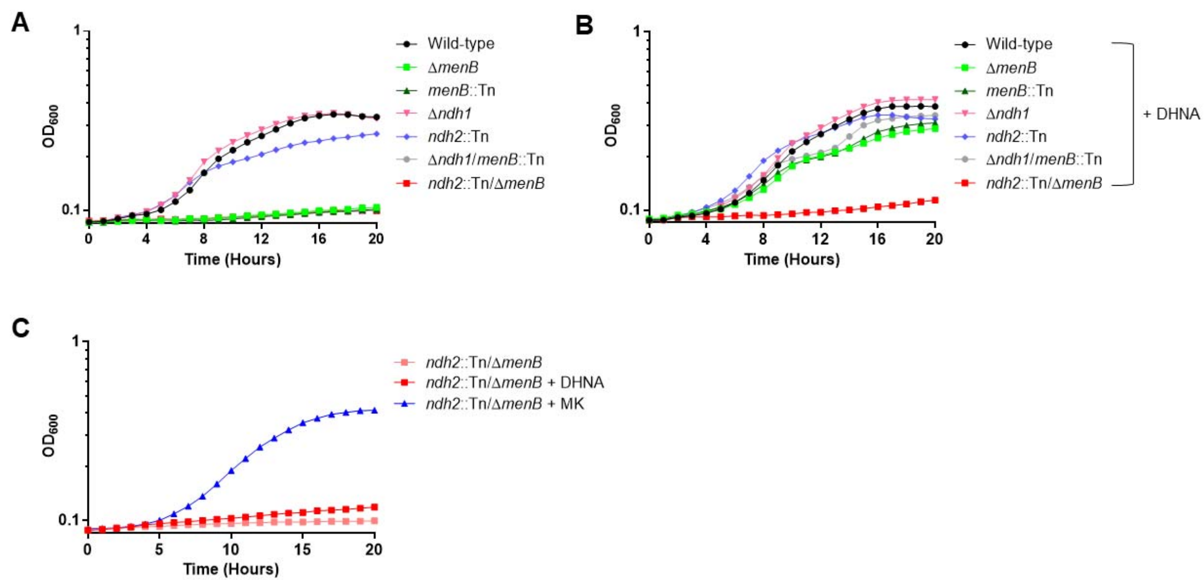

412

413 **Figure 4.** *ndh2* is conditionally essential for DHNA utilization *in vitro*. Indicated strains of
414 *L. monocytogenes* were grown in defined medium without (A) or with (B) 5µM DHNA
415 supplementation aerobically at 37°C and monitored for OD_{600} over 20 hr. (C)
416 *ndh2*::Tn/Δ*menB L. monocytogenes* was grown aerobically in defined medium with
417 either 5µM DHNA or 5µM MK and monitored for growth (OD_{600}) over 20 hr. All data
418 represent one representative out of three biological replicates.

419

420

bioRxiv preprint doi: https://doi.org/10.1101/2023.01.13.524026; this version posted January 14, 2023. The copyright holder for this preprint (which was not certified by peer review) is the author/funder, who has granted bioRxiv a license to display the preprint in perpetuity. It is made available under aCC-BY-NC-ND 4.0 International license.

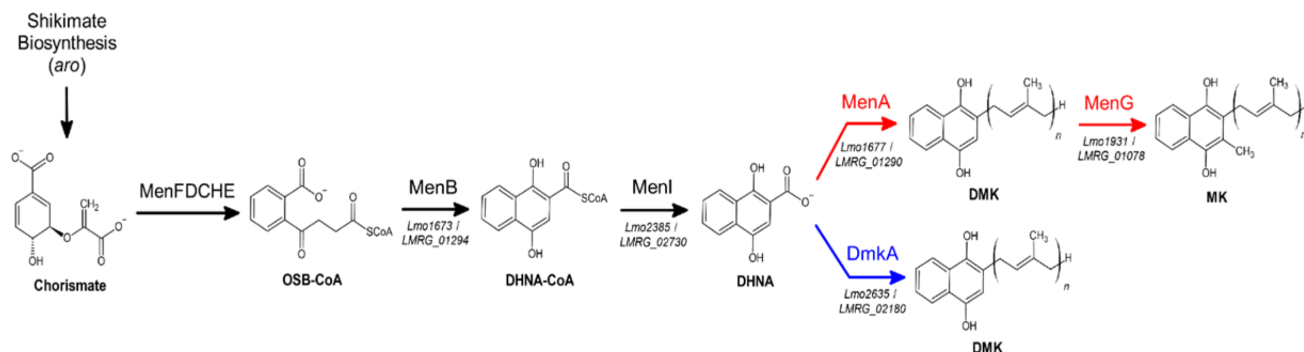

421
422 **Figure S1.** Menaquinone biosynthetic pathway in *Listeria monocytogenes*. Chorismate
423 is generated by the upstream shikimate biosynthesis pathway and is converted to
424 DHNA by the series of listed enzymes (MenFDCHEBI). Red arrows indicate DHNA
425 branching point towards aerobic respiration. Blue arrow indicates DHNA branching point
426 towards anaerobic respiration. Corresponding gene locus numbers for *L.*
427 *monocytogenes* strains EGD-e (*Lmo*) and 10403S (*LMRG*; parental strain used in this
428 study) are listed underneath reaction arrows. OSB, *o*-succinylbenzoate; DMK,
429 demethylmenaquinone.
430
431
432

bioRxiv preprint doi: https://doi.org/10.1101/2023.01.13.524026; this version posted January 14, 2023. The copyright holder for this preprint (which was not certified by peer review) is the author/funder, who has granted bioRxiv a license to display the preprint in perpetuity. It is made available under aCC-BY-NC-ND 4.0 International license.

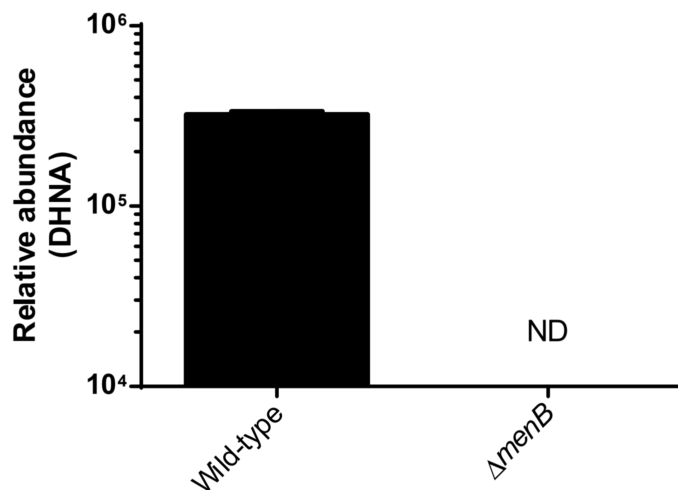

433

434 **Figure S2.** Detection of secreted DHNA by mass spectrometry. Detection of DHNA
435 from the cell-free supernatants of overnight aerobic cultures of wildtype or Δ*menB*
436 strains by mass spectrometry. Data were analyzed via MAVEN. Error bars represent the
437 standard deviation of the means from two independent experiments.

438

439

440

441

442

bioRxiv preprint doi: https://doi.org/10.1101/2023.01.13.524026; this version posted January 14, 2023. The copyright holder for this preprint (which was not certified by peer review) is the author/funder, who has granted bioRxiv a license to display the preprint in perpetuity. It is made available under aCC-BY-NC-ND 4.0 International license.

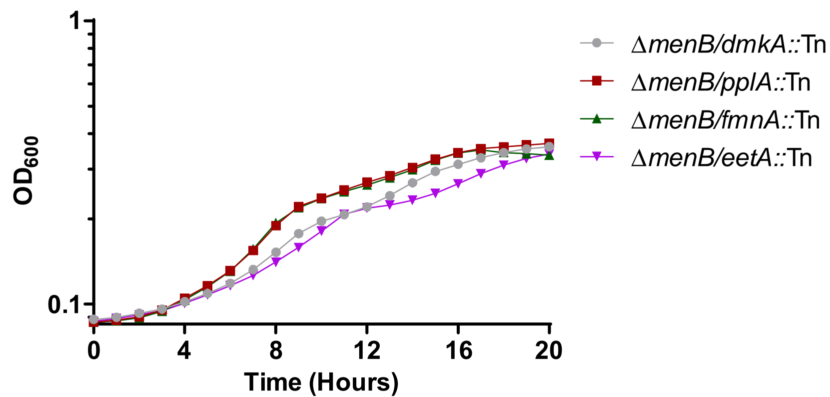

443

444 **Figure S3.** Four separate genes other than *ndh2* that are part of the *L. monocytogenes*
445 EET locus did not display growth defects. Indicated strains were grown in defined
446 medium at 37°C with the addition of 5μM DHNA. OD_{600} was monitored for 20 hours.
447 Data represents one representative out of three biological replicates.

448

449

450

451

452

453

454

455

456

457

458

459

460

bioRxiv preprint doi: https://doi.org/10.1101/2023.01.13.524026; this version posted January 14, 2023. The copyright holder for this preprint (which was not certified by peer review) is the author/funder, who has granted bioRxiv a license to display the preprint in perpetuity. It is made available under aCC-BY-NC-ND 4.0 International license.

461 **MATERIALS AND METHODS**

462 **Bacterial strains, plasmid construction, and growth conditions *in vitro*.** *L.*
463 *monocytogenes* strain 10403S is referred to as the wild-type strain, and all other strains
464 used in this study are isogenic derivatives of this parental strain. Vectors were
465 conjugated into *L. monocytogenes* by *Escherichia coli* strain S17 or SM10 (47). The
466 integrative vector pIMK2 was used for constitutive expression of *L. monocytogenes*
467 genes for complementation (48).

468 *L. monocytogenes* strains were grown at 37°C or 30°C in brain heart infusion
469 (BHI) medium (237500; VWR) or defined medium supplemented with glucose as the
470 sole carbon source. Defined medium is identical to the formulation described by Smith
471 *et al.* (220). *Escherichia coli* strains were grown in Luria-Bertani (LB) broth at 37°C.
472 Antibiotics were used at concentrations of 100 µg/ml carbenicillin (IB02020; IBI
473 Scientific), 10 µg/ml chloramphenicol (190321; MP Biomedicals), 2 µg/ml erythromycin
474 (227330050; Acros Organics), or 30 µg/ml kanamycin (BP906-5; Fisher Scientific) when
475 appropriate. Medium, where indicated, was supplemented with 5 µM 1,4-dihydroxy-2-
476 naphthoate (DHNA) (281255; Sigma) or 5 µM menaquinone (MK) (V9378; Sigma).
477

478 **Phage Transduction**

479 Phage transductions were performed as previously described (310). Briefly, MACK *L.*
480 *monocytogenes* was grown overnight in 3mL LB at 30°C stationary to propagate U153
481 phage stocks. MACK cultures were pelleted and resuspended in LB + 10mM $CaSO_4$ +
482 10mM $MgCl_2$ and added into LB + 0.7% agar + 10mM $CaSO_4$ + 10mM $MgCl_2$ at 42°C.
483 This mixture was immediately poured on BHI plates and incubated overnight at 30°C.

bioRxiv preprint doi: https://doi.org/10.1101/2023.01.13.524026; this version posted January 14, 2023. The copyright holder for this preprint (which was not certified by peer review) is the author/funder, who has granted bioRxiv a license to display the preprint in perpetuity. It is made available under aCC-BY-NC-ND 4.0 International license.

484 U153 phage plaques were collected and soaked out with 10mM Tris (pH7.5) + 10mM
485 $CaSO_4$ + 10mM $MgCl_2$. Donor plaque soak-outs were propagated the same way and
486 were filter-sterilized using a 0.2μm syringe filter (09-740-113; Fisher Scientific) and
487 additionally kept sterile by adding 500μL chloroform. Recipient Δ*menB* strain was
488 infected with these donor soak-outs for 30 minutes at room temperature and
489 subsequently plated on BHI agar with erythromycin for selection at 37°C.
490
491 **Intracellular bacteriolysis assay.** Standard intracellular bacteriolysis assays were
492 performed as previously described (29). Briefly, primary or immortalized bone marrow-
493 derived *IFNAR*$^{-/-}$ macrophages (5×10^5 per well of 24-well plates) were grown in a
494 monolayer overnight in 500 μL volume. *L. monocytogenes* strains carrying the
495 bacteriolysis reporter pBHE573 (35) were grown at 30°C without shaking overnight.
496 Cultures were then diluted to a final concentration of 5×10^8 CFU/mL in PBS and used
497 to infect macrophages at a MOI of 10. At 1 hr postinfection, media were removed and
498 replaced with media containing 50 μg/ml gentamicin. At 6 hr post infection, media from
499 the wells were aspirated and macrophages were lysed using TNT lysis buffer (20 mM
500 Tris, 200 mM NaCl, 1% Triton [pH 8.0]). Cell lysates were transferred to opaque 96-well
501 plates, and luciferin reagent was added and assayed for luciferase activity (Synergy HT,
502 BioTek; Winooski, VT).
503
504 **Intracellular growth assay.** Bone marrow-derived macrophages (BMDMs) were
505 prepared from C57BL/6 mice as previously described (51). BMDMs were plated on
506 coverslips at 5×10^6 cells per 60mm dish and allowed to adhere overnight. BMDMs

bioRxiv preprint doi: https://doi.org/10.1101/2023.01.13.524026; this version posted January 14, 2023. The copyright holder for this preprint (which was not certified by peer review) is the author/funder, who has granted bioRxiv a license to display the preprint in perpetuity. It is made available under aCC-BY-NC-ND 4.0 International license.

507 were then infected at an MOI of 0.2 with their respective strain and infection proceeded
508 for 8 hr. At 30 min postinfection, media were removed and replaced with media
509 containing 50 µg/ml gentamicin. Total CFU were quantified at various time points as
510 previously described (50).
511
512 **NAD^+ and NADH measurements.** *L. monocytogenes* strains were grown in defined
513 medium at 37°C with shaking to mid-logarithmic phase (OD_{600} 0.4-0.6). Cultures were
514 centrifuged and then resuspended in PBS. Resuspended bacteria were then lysed
515 (2×10^8 total CFU) by a 1:1 addition of 1% dodecyltrimethylammonium bromide
516 (DTAB) (AC409310250; Fisher Scientific) for 5 min with agitation. Lysates were then
517 processed to measure NAD^+ and NADH levels using the NAD/NADH-Glo assay
518 (Promega, G9071) per the manufacturer's protocol.
519
520 **Fermentation byproduct measurements.** Cultures of *L. monocytogenes* were grown
521 in BHI at 37°C with shaking overnight. Bacteria were then centrifuged and 1 mL of the
522 resulting supernatant was filtered through a 0.2µm-pore-size syringe filter (09-740-113;
523 Fisher Scientific). Supernatant samples were next treated with 2µL of H_2SO_4 to
524 precipitate any components that might be incompatible with the running buffer. The
525 samples were then centrifuged at 16000 × g for 10 min and then 200µL of each sample
526 transferred to an HPLC vial. HPLC analysis was performed using a ThermoFisher
527 (Waltham, MA) Ultimate 3000 UHPLC system equipped with a UV detector (210 nm).
528 Compounds were separated on a 250 × 4.6 mm Rezex© ROA-Organic acid LC column
529 (Phenomenex Torrance, CA) run with a flow rate of 0.2 mL min^{-1} and at a column

bioRxiv preprint doi: https://doi.org/10.1101/2023.01.13.524026; this version posted January 14, 2023. The copyright holder for this preprint (which was not certified by peer review) is the author/funder, who has granted bioRxiv a license to display the preprint in perpetuity. It is made available under aCC-BY-NC-ND 4.0 International license.

530 temperature of 50 °C. The samples were held at 4 °C prior to injection. Separation was
531 isocratic with a mobile phase of HPLC grade water acidified with 0.015 N H_2SO_4 (415
532 μL L^{-1}). At least two standard sets were run along with each sample set. Standards
533 were 100, 20, 4, and 0.8mM concentrations of lactate or acetate. The resultant data was
534 analyzed using the Thermofisher Chromeleon 7 software package.
535
536 **Acute virulence assay.** All techniques were reviewed and approved by the University
537 of Wisconsin — Madison Institutional Animal Care and Use Committee (IACUC) under
538 the protocol M02501. Female C57BL/6 mice (6 to 8 weeks of age; purchased from
539 Charles River) were used for the purposes of this study. *L. monocytogenes* strains were
540 grown in BHI medium at 30°C without shaking overnight. These cultures were then
541 back-diluted the following day 1:5 into fresh BHI medium and grown at 37°C with
542 shaking until mid-exponential phase (OD_{600} 0.4-0.6). Bacteria were diluted in PBS to a
543 concentration of 5×10^5 CFU/mL and mice were injected intravenously with 1×10^5
544 total CFU. At 48 hr postinfection, spleens and livers were harvested and homogenized
545 in 0.1% Nonidet P-40 in PBS. Homogenates were then plated on LB plates to
546 enumerate CFU and quantify bacterial burdens.
547
548 **Statistical analysis.** Statistical significance analysis (GraphPad Prism, version 6.0h)
549 was determined by one-way analysis of variance (ANOVA) with a Dunnett's posttest
550 comparing wild-type to all other indicated strains or by one-way ANOVA with Tukey's
551 multiple comparisons test unless otherwise stated (*, $P \leq 0.05$; **, $P \leq 0.01$; ***, $P \leq$
552 0.001; ****, $P \leq 0.0001$).

bioRxiv preprint doi: https://doi.org/10.1101/2023.01.13.524026; this version posted January 14, 2023. The copyright holder for this preprint (which was not certified by peer review) is the author/funder, who has granted bioRxiv a license to display the preprint in perpetuity. It is made available under aCC-BY-NC-ND 4.0 International license.

553 **ACKNOWLEDGEMENTS**

554 We would like to thank Dr. Samuel Light for providing the vector pPL2-NOX, expressing
555 the water-forming NADH oxidase for integration into *Listeria monocytogenes*.

556

557 **FUNDING INFORMATION**

558 This work was funded by the National Institutes of Health (T32007215 [HBS] and
559 R01AI137070 [J-D S]). The funders had no role in study design, data collection and
560 interpretation, or the decision to submit the work for publication.

561
562
563
564
565
566
567
568
569
570
571
572
573
574

bioRxiv preprint doi: https://doi.org/10.1101/2023.01.13.524026; this version posted January 14, 2023. The copyright holder for this preprint (which was not certified by peer review) is the author/funder, who has granted bioRxiv a license to display the preprint in perpetuity. It is made available under aCC-BY-NC-ND 4.0 International license.

575 **Table S3.1** Strains used in this study.
576

Strain	Description	Reference
XL1-Blue	Competent *E. coli* strain	-
SM10	*E. coli* strain for conjugations into *Lm;* Km^R	(47)
10403S	Parental *L. monocytogenes* (*Lm*) 10403s strain [Wild-type]	-
JDS18	*Lm* with pBHE573	(35)
HS28	*Lm* with pPL2-NOX	(34)
JDS2328	*Lm* with pBHE573 and pPL2-NOX	(34)
JDS25	*Lm* Δ*glmR*	(35)
JDS21	*Lm* Δ*glmR* with pBHE573	(35)
JDS2327	*Lm* Δ*glmR* with pPL2-NOX	This work
JDS2329	*Lm* Δ*glmR* with pBHE573 and pPL2-NOX	(34)
JDS1161	*Lm* Δ*menB*	(29)
JDS1175	*Lm* Δ*menB* with pYL116	(32)
JDS1958	*Lm* Δ*menB* with pPL2-NOX	(34)
JDS1191	*Lm* Δ*menB* with pBHE573	(29)
JDS2333	*Lm* Δ*menB* with pBHE573 and pPL2-NOX	(34)
JDS2240	*Lm* Δ*menI*	(32)
JDS2155	*Lm* Δ*menI* with pBHE573	(32)
JDS2325	*Lm* Δ*menI* with pPL2-NOX	This work
JDS2326	*Lm* Δ*menI* with pBHE573 and pPL2-NOX	This work
JDS1047	*Lm* Δ*menA*	(29)
JDS813	*Lm* Δ*menA* with pBHE573	(29)
HS30	*Lm* Δ*menA* with pPL2-NOX	This work
JDS2330	*Lm* Δ*menA* with pBHE573 and pPL2-NOX	This work
JDS1213	*Lm* Δ*menD*	(52)
JDS17	SM10 *E. coli* with pBHE537	(35)
JDS1957	SM10 *E. coli* with pPL2-NOX	(34)
KL1	*Lm* Δ*ndh1*/*menB*::Tn	This work
KL4	*Lm* Δ*menB*/*ndh2*::Tn	This work
KL9	*Lm* Δ*menB*/*dmkA*::Tn	This work
KL10	*Lm* Δ*menB*/*pplA*::Tn	This work
KL11	*Lm* Δ*menB*/*fmnA*::Tn	This work
KL12	*Lm* Δ*menB*/*eetA*::Tn	This work

577

578

bioRxiv preprint doi: https://doi.org/10.1101/2023.01.13.524026; this version posted January 14, 2023. The copyright holder for this preprint (which was not certified by peer review) is the author/funder, who has granted bioRxiv a license to display the preprint in perpetuity. It is made available under aCC-BY-NC-ND 4.0 International license.

579 **Table S3.2** Plasmids used in this study.

Plasmids	Description	Reference
pBHE573	Bacteriolysis reporter; Cam^R	(35)
pIMK2	Constitutive expression vector for complementation, P_{help}; Kan^R	(48)
pYL116	*menB* cloned into pIMK2	(32)
pPL2-NOX	NADH oxidase (NOX) cloned into the backbone of pPL2	(34)

580
581
582
583
584
585
586
587
588
589
590
591
592
593
594
595
596
597

bioRxiv preprint doi: https://doi.org/10.1101/2023.01.13.524026; this version posted January 14, 2023. The copyright holder for this preprint (which was not certified by peer review) is the author/funder, who has granted bioRxiv a license to display the preprint in perpetuity. It is made available under aCC-BY-NC-ND 4.0 International license.

598 **References**

599 1. Goetz M, Bubert A, Wang G, Chico-Calero I, Vazquez-Boland JA, Beck M,
600 Slaghuis J, Szalay AA, Goebel W. Microinjection and growth of bacteria in the
601 cytosol of mammalian host cells. Proc Natl Acad Sci U S A. 2001 Oct
602 9;98(21):12221-6. doi: 10.1073/pnas.211106398.
603 2. Freitag NE, Port GC, Miner MD. Listeria monocytogenes - from saprophyte to
604 intracellular pathogen. Nat Rev Microbiol. 2009 Sep;7(9):623-8. doi:
605 10.1038/nrmicro2171.
606 3. Ray K, Marteyn B, Sansonetti PJ, Tang CM. Life on the inside: the intracellular
607 lifestyle of cytosolic bacteria. Nat Rev Microbiol. 2009 May;7(5):333-40. doi:
608 10.1038/nrmicro2112.
609 4. Beuzón CR, Salcedo SP, Holden DW. Growth and killing of a Salmonella
610 enterica serovar Typhimurium sifA mutant strain in the cytosol of different host
611 cell lines. Microbiology. 2002;148. doi:10.1099/00221287-148-9-2705.
612 5. Brumell JH, Rosenberger CM, Gotto GT, Marcus SL, Finlay BB. SifA permits
613 survival and replication of Salmonella typhimurium in murine macrophages. Cell
614 Microbiol. 2001 Feb;3(2):75-84. doi:10.1046/j.1462-5822.2001.00087.x.
615 6. Laguna RK, Creasey EA, Li Z, Valtz N, Isberg RR. A Legionella pneumophila-
616 translocated substrate that is required for growth within macrophages and
617 protection from host cell death. Proc Natl Acad Sci U S A. 2006;103.
618 doi:10.1073/pnas.0609012103.
619 7. Slaghuis J, Goetz M, Engelbrecht F, Goebel W. Inefficient replication of Listeria
620 innocua in the cytosol of mammalian cells. J Infect Dis. 2004 Feb 1;189(3):393-
621 401. doi: 10.1086/381206.
622 8. Zhang Y, Yeruva L, Marinov A, Prantner D, Wyrick PB, Lupashin V, et al. The
623 DNA Sensor, Cyclic GMP–AMP Synthase, Is Essential for Induction of IFN-β
624 during Chlamydia trachomatis Infection. The Journal of Immunology. 2014;193.
625 doi:10.4049/jimmunol.1302718.
626 9. Ge J, Gong Y-N, Xu Y, Shao F. Preventing bacterial DNA release and absent in
627 melanoma 2 inflammasome activation by a Legionella effector functioning in
628 membrane trafficking. Proc Natl Acad Sci U S A. 2012;109.
629 doi:10.1073/pnas.1117490109
630 10. Collins AC, Cai H, Li T, Franco LH, Li X-D, Nair VR, et al. Cyclic GMP-AMP
631 Synthase Is an Innate Immune DNA Sensor for Mycobacterium tuberculosis. Cell
632 Host & Microbe. 2015;17. doi:10.1016/j.chom.2015.05.005
633 11. Watson RO, Bell SL, MacDuff DA, Kimmey JM, Diner EJ, Olivas J, et al. The
634 Cytosolic Sensor cGAS Detects Mycobacterium tuberculosis DNA to Induce
635 Type I Interferons and Activate Autophagy. Cell Host & Microbe. 2015;17.
636 doi:10.1016/j.chom.2015.05.004
637 12. Wassermann R, Gulen MF, Sala C, Perin SG, Lou Y, Rybniker J, et al.
638 Mycobacterium tuberculosis Differentially Activates cGAS- and Inflammasome-

bioRxiv preprint doi: https://doi.org/10.1101/2023.01.13.524026; this version posted January 14, 2023. The copyright holder for this preprint (which was not certified by peer review) is the author/funder, who has granted bioRxiv a license to display the preprint in perpetuity. It is made available under aCC-BY-NC-ND 4.0 International license.

639 Dependent Intracellular Immune Responses through ESX-1. Cell Host &
640 Microbe. 2015;17. doi:10.1016/j.chom.2015.05.003
641 13. McNab, F., Mayer-Barber, K., Sher, A. et al. Type I interferons in infectious
642 disease. Nat Rev Immunol 15, 87–103 (2015). https://doi.org/10.1038/nri3787
643 14. Portnoy DA, Auerbuch V, Glomski IJ. The cell biology of Listeria monocytogenes
644 infection: the intersection of bacterial pathogenesis and cell-mediated immunity. J
645 Cell Biol. 2002 Aug 5;158(3):409-14. doi: 10.1083/jcb.200205009.
646 15. Vázquez-Boland JA, Kuhn M, Berche P, Chakraborty T, Domínguez-Bernal G,
647 Goebel W, González-Zorn B, Wehland J, Kreft J. Listeria pathogenesis and
648 molecular virulence determinants. Clin Microbiol Rev. 2001 Jul;14(3):584-640.
649 doi: 10.1128/CMR.14.3.584-640.2001.
650 16. Portnoy DA, Jacks PS, Hinrichs DJ. Role of hemolysin for the intracellular growth
651 of Listeria monocytogenes. J Exp Med. 1988 Apr 1;167(4):1459-71. doi:
652 10.1084/jem.167.4.1459.
653 17. Tilney LG, Portnoy DA. Actin filaments and the growth, movement, and spread of
654 the intracellular bacterial parasite, Listeria monocytogenes. J Cell Biol. 1989
655 Oct;109(4 Pt 1):1597-608. doi: 10.1083/jcb.109.4.1597.
656 18. Brundage RA, Smith GA, Camilli A, Theriot JA, Portnoy DA. Expression and
657 phosphorylation of the Listeria monocytogenes ActA protein in mammalian cells.
658 Proc Natl Acad Sci U S A. 1993 Dec 15;90(24):11890-4. doi:
659 10.1073/pnas.90.24.11890.
660 19. Moors MA, Levitt B, Youngman P, Portnoy DA. Expression of listeriolysin O and
661 ActA by intracellular and extracellular Listeria monocytogenes. Infect Immun.
662 1999 Jan;67(1):131-9. doi: 10.1128/IAI.67.1.131-139.1999.
663 20. Shetron-Rama LM, Marquis H, Bouwer HG, Freitag NE. Intracellular induction of
664 Listeria monocytogenes actA expression. Infect Immun. 2002 Mar;70(3):1087-96.
665 doi: 10.1128/IAI.70.3.1087-1096.2002.
666 21. Smith GA, Marquis H, Jones S, Johnston NC, Portnoy DA, Goldfine H. The two
667 distinct phospholipases C of Listeria monocytogenes have overlapping roles in
668 escape from a vacuole and cell-to-cell spread. Infect Immun. 1995
669 Nov;63(11):4231-7. doi: 10.1128/iai.63.11.4231-4237.1995.
670 22. Sauer JD, Herskovits AA, O'Riordan MXD. Metabolism of the Gram-Positive
671 Bacterial Pathogen Listeria monocytogenes. Microbiol Spectr. 2019
672 Jul;7(4):10.1128/microbiolspec.GPP3-0066-2019. doi:
673 10.1128/microbiolspec.GPP3-0066-2019.
674 23. P G, L F, C B, C R, A A, F B, P B, H B, P B, T C, A C, F C, E C, A de D, P D, E
675 D, G D-B, E D, L D, O D, KD E, H F, F GP, P G, L G, W G, N G-L, T H, J H, D J,
676 LM J, U K, J K, M K, F K, G K, E M, A M, JM V, E N, H N, G N, S N, B de P, JC
677 P-D, R P, B R, M R, T S, N S, A T, JA V-B, H V, J W, P C. 2001. Comparative
678 genomics of Listeria species. Science. 2001 Oct 26;294(5543):849-52. doi:
679 10.1126/science.1063447.

bioRxiv preprint doi: https://doi.org/10.1101/2023.01.13.524026; this version posted January 14, 2023. The copyright holder for this preprint (which was not certified by peer review) is the author/funder, who has granted bioRxiv a license to display the preprint in perpetuity. It is made available under aCC-BY-NC-ND 4.0 International license.

680 24. Romick TL, Fleming HP, McFeeters RF. Aerobic and anaerobic metabolism of
681 Listeria monocytogenes in defined glucose medium. Appl Environ Microbiol.
682 1996 Jan;62(1):304-7. doi: 10.1128/aem.62.1.304-307.1996.
683 25. Light SH, Su L, Rivera-Lugo R, Cornejo JA, Louie A, Iavarone AT, Ajo-Franklin
684 CM, Portnoy DA. A flavin-based extracellular electron transfer mechanism in
685 diverse Gram-positive bacteria. Nature. 2018 Oct;562(7725):140-144. doi:
686 10.1038/s41586-018-0498-z.
687 26. Meganathan R. Biosynthesis of menaquinone (vitamin K2) and ubiquinone
688 (coenzyme Q): a perspective on enzymatic mechanisms. Vitam Horm.
689 2001;61:173-218. doi: 10.1016/s0083-6729(01)61006-9.
690 27. Corbett D, Goldrick M, Fernandes VE, Davidge K, Poole RK, Andrew PW, Cavet
691 J, Roberts IS. Listeria monocytogenes Has Both Cytochrome bd-Type and
692 Cytochrome aa3-Type Terminal Oxidases, Which Allow Growth at Different
693 Oxygen Levels, and Both Are Important in Infection. Infect Immun. 2017 Oct
694 18;85(11):e00354-17. doi: 10.1128/IAI.00354-17.
695 28. Light SH, Méheust R, Ferrell JL, Cho J, Deng D, Agostoni M, Iavarone AT,
696 Banfield JF, D'Orazio SEF, Portnoy DA. 2019. Extracellular electron transfer
697 powers flavinylated extracellular reductases in Gram-positive bacteria. Proc Natl
698 Acad Sci U S A 116:26892–26899.
699 29. Chen, G.Y., McDougal, C.E., D'Antonio, M.A., Portman, J.L. and Sauer, JD. A
700 Genetic Screen Reveals that Synthesis of 1,4-Dihydroxy-2-Naphthoate (DHNA),
701 but Not Full-Length Menaquinone, Is Required for Listeria monocytogenes
702 Cytosolic Survival. MBio. 2017 Mar 21;8(2).
703 30. Stritzker J, Janda J, Schoen C, Taupp M, Pilgrim S, Gentschev I, Schreier P,
704 Geginat G, Goebel W. Growth, virulence, and immunogenicity of Listeria
705 monocytogenes aro mutants. Infect Immun. 2004 Oct;72(10):5622-9. doi:
706 10.1128/IAI.72.10.5622-5629.2004.
707 31. Chen GY, Kao CY, Smith HB, Rust DP, Powers ZM, Li AY, Sauer JD. Mutation of
708 the Transcriptional Regulator YtoI Rescues Listeria monocytogenes Mutants
709 Deficient in the Essential Shared Metabolite 1,4-Dihydroxy-2-Naphthoate
710 (DHNA). Infect Immun. 2019 Dec 17;88(1):e00366-19. doi: 10.1128/IAI.00366-
711 19.
712 32. Smith HB, Li TL, Liao MK, Chen GY, Guo Z, Sauer JD. Listeria monocytogenes
713 MenI Encodes a DHNA-CoA Thioesterase Necessary for Menaquinone
714 Biosynthesis, Cytosolic Survival, and Virulence. Infect Immun. 2021 Apr
715 16;89(5):e00792-20. doi: 10.1128/IAI.00792-20.
716 33. Pensinger DA, Gutierrez K V., Smith HB, Vincent WJB, Stevenson DS, Black KA,
717 Perez-Medina KM, Dillard JP, Rhee KY, Amador-Noguez D, Huynh TN, Sauer J-
718 D. 2021. Listeria monocytogenes GlmR is an accessory uridyltransferase
719 essential for cytosolic survival and virulence. bioRxiv.
720 https://doi.org/10.1101/2021.10.27.466214.
721 34. Rivera-Lugo R, Deng D, Anaya-Sanchez A, Tejedor-Sanz S, Tang E, Reyes Ruiz
722 VM, Smith HB, Titov DV, Sauer JD, Skaar EP, Ajo-Franklin CM, Portnoy DA,

bioRxiv preprint doi: https://doi.org/10.1101/2023.01.13.524026; this version posted January 14, 2023. The copyright holder for this preprint (which was not certified by peer review) is the author/funder, who has granted bioRxiv a license to display the preprint in perpetuity. It is made available under aCC-BY-NC-ND 4.0 International license.

723 Light SH. Listeria monocytogenes requires cellular respiration for NAD^+
724 regeneration and pathogenesis. Elife. 2022 Apr 5;11:e75424. doi:
725 10.7554/eLife.75424.
726 35. Sauer JD, Witte CE, Zemansky J, Hanson B, Lauer P, Portnoy DA. Listeria
727 monocytogenes triggers AIM2-mediated pyroptosis upon infrequent bacteriolysis
728 in the macrophage cytosol. Cell Host Microbe. 2010 May 20;7(5):412-9. doi:
729 10.1016/j.chom.2010.04.004.
730 36. Pensinger DA, Boldon KM, Chen GY, Vincent WJ, Sherman K, Xiong M,
731 Schaenzer AJ, Forster ER, Coers J, Striker R, Sauer JD. The Listeria
732 monocytogenes PASTA Kinase PrkA and Its Substrate YvcK Are Required for
733 Cell Wall Homeostasis, Metabolism, and Virulence. PLoS Pathog. 2016 Nov
734 2;12(11):e1006001. doi: 10.1371/journal.ppat.1006001.
735 37. Hunt KA, Flynn JM, Naranjo B, Shikhare ID, Gralnick JA. Substrate-level
736 phosphorylation is the primary source of energy conservation during anaerobic
737 respiration of Shewanella oneidensis strain MR-1. J Bacteriol. 2010
738 Jul;192(13):3345-51. doi: 10.1128/JB.00090-10. Epub 2010 Apr 16.
739 38. Mevers E, Su L, Pishchany G, Baruch M, Cornejo J, Hobert E, Dimise E, Ajo-
740 Franklin CM, Clardy J. An elusive electron shuttle from a facultative anaerobe.
741 Elife. 2019 Jun 24;8:e48054. doi: 10.7554/eLife.48054.
742 39. Brutinel ED, Gralnick JA. Shuttling happens: soluble flavin mediators of
743 extracellular electron transfer in Shewanella. Appl Microbiol Biotechnol. 2012
744 Jan;93(1):41-8. doi: 10.1007/s00253-011-3653-0.
745 40. Tejedor-Sanz S, Stevens ET, Li S, Finnegan P, Nelson J, Knoesen A, Light SH,
746 Ajo-Franklin CM, Marco ML. Extracellular electron transfer increases
747 fermentation in lactic acid bacteria via a hybrid metabolism. Elife. 2022 Feb
748 11;11:e70684. doi: 10.7554/eLife.70684.
749 41. Wang Y, Kern SE, Newman DK. Endogenous phenazine antibiotics promote
750 anaerobic survival of Pseudomonas aeruginosa via extracellular electron
751 transfer. J Bacteriol. 2010 Jan;192(1):365-9. doi: 10.1128/JB.01188-09.
752 42. Rabaey K, Boon N, Höfte M, Verstraete W. Microbial phenazine production
753 enhances electron transfer in biofuel cells. Environ Sci Technol. 2005 May
754 1;39(9):3401-8. doi: 10.1021/es048563o.
755 43. Isawa K, Hojo K, Yoda N, Kamiyama T, Makino S, Saito M, Sugano H, Mizoguchi
756 C, Kurama S, Shibasaki M, Endo N, Sato Y. Isolation and identification of a new
757 bifidogenic growth stimulator produced by Propionibacterium freudenreichii ET-3.
758 Biosci Biotechnol Biochem. 2002 Mar;66(3):679-81. doi: 10.1271/bbb.66.679.
759 44. Franza T, Delavenne E, Derré-Bobillot A, Juillard V, Boulay M, Demey E, Vinh J,
760 Lamberet G, Gaudu P. A partial metabolic pathway enables group b
761 streptococcus to overcome quinone deficiency in a host bacterial community. Mol
762 Microbiol. 2016 Oct;102(1):81-91. doi: 10.1111/mmi.13447.
763 45. Kang JE, Kim TJ, Moon GS. A Novel Lactobacillus casei LP1 Producing 1,4-
764 Dihydroxy-2-Naphthoic Acid, a Bifidogenic Growth Stimulator. Prev Nutr Food
765 Sci. 2015 Mar;20(1):78-81. doi: 10.3746/pnf.2015.20.1.78.

bioRxiv preprint doi: https://doi.org/10.1101/2023.01.13.524026; this version posted January 14, 2023. The copyright holder for this preprint (which was not certified by peer review) is the author/funder, who has granted bioRxiv a license to display the preprint in perpetuity. It is made available under aCC-BY-NC-ND 4.0 International license.

766 46. Grubmüller S, Schauer K, Goebel W, Fuchs TM, Eisenreich W. Analysis of
767 carbon substrates used by Listeria monocytogenes during growth in J774A.1
768 macrophages suggests a bipartite intracellular metabolism. Front Cell Infect
769 Microbiol. 2014 Nov 3;4:156. doi: 10.3389/fcimb.2014.00156.
770 47. Simon, R., Priefer, U. and Pühler, A. A Broad Host Range Mobilization System
771 for in Vivo Genetic Engineering: Transposon Mutagenesis in Gram Negative
772 Bacteria. Nature Biotechnology, 1983, 1, 784-791.
773 http://dx.doi.org/10.1038/nbt1183-784
774 48. Monk IR, Gahan CG, Hill C. Tools for functional postgenomic analysis of listeria
775 monocytogenes. Appl Environ Microbiol. 2008 Jul;74(13):3921-34. doi:
776 10.1128/AEM.00314-08. Epub 2008 Apr 25.
777 49. Hodgson DA. Generalized transduction of serotype 1/2 and serotype 4b strains
778 of Listeria monocytogenes. Mol Microbiol. 2000 Jan;35(2):312-23. doi:
779 10.1046/j.1365-2958.2000.01643.x.
780 50. Rohmer L, Hocquet D, Miller SI. Are pathogenic bacteria just looking for food?
781 Metabolism and microbial pathogenesis. Trends Microbiol. 2011 Jul;19(7):341-8.
782 doi: 10.1016/j.tim.2011.04.003. Epub 2011 May 18.
783 51. Jones S, Portnoy DA. Characterization of Listeria monocytogenes pathogenesis
784 in a strain expressing perfringolysin O in place of listeriolysin O. Infect Immun.
785 1994 Dec;62(12):5608-13. doi: 10.1128/iai.62.12.5608-5613.1994.
786 52. Perry KJ, Higgins DE. A differential fluorescence-based genetic screen identifies
787 Listeria monocytogenes determinants required for intracellular replication. J
788 Bacteriol. 2013 Aug;195(15):3331-40. doi: 10.1128/JB.00210-13.
789 53. Lencina AM, Franza T, Sullivan MJ, Ulett GC, Ipe DS, Gaudu P, Gennis RB,
790 Schurig-Briccio LA. Type 2 NADH Dehydrogenase Is the Only Point of Entry for
791 Electrons into the Streptococcus agalactiae Respiratory Chain and Is a Potential
792 Drug Target. mBio. 2018 Jul 3;9(4):e01034-18. doi: 10.1128/mBio.01034-18.
793